Stereo Day-for-Night: Retargeting Disparity for Scotopic Vision

PETR KELLNHOFER, MPI Informatik, Germany
TOBIAS RITSCHEL, MPI Informatik and Saarland University, Germany
PETER VANGORP, MPI Informatik, Germany
KAROL MYSZKOWSKI, MPI Informatik, Germany
HANS-PETER SEIDEL, MPI Informatik, Germany

Several approaches attempt to reproduce the appearance of a scotopic low-light night scene on a photopic display ("day-for-night") by introducing color desaturation, loss of acuity and the Purkinje shift towards blue colors. We argue that faithful stereo reproduction of night scenes on photopic stereo displays requires manipulation of not only color but also binocular disparity. To this end, we performed a psychophysics experiment to devise a model of disparity at scotopic luminance levels. Using this model, we can match binocular disparity of a scotopic stereo content displayed on a photopic monitor to the disparity that would be perceived if the scene was actually scotopic. The model allows for real-time computation of common stereo content as found in interactive applications such as simulators or computer games.

Categories and Subject Descriptors: I.3.3 [**Computer Graphics**]: Picture/Image Generation—*Viewing algorithms*; I.3.8 [**Computer Graphics**] Applications

General Terms: Human factors

Additional Key Words and Phrases: Night vision, scotopic vision, stereoscopic 3D

ACM Reference Format:

Kellnhofer, P. and Ritschel, T. and Vangorp, P. and Myszkowski, K. and Seidel, H.-P. 2014. Stereo Day-for-Night: Retargeting Disparity for Scotopic Vision. ACM Trans. Appl. Percept. 11, 3, Article 15 (August 2014), 17 pages.
DOI = 10.1145/2644813 http://doi.acm.org/10.1145/2644813

1. INTRODUCTION

The change of appearance between the same scene presented once at photopic luminance adaptation levels (daylight) and once at scotopic conditions (night vision) is not limited to a simple decrease of brightness but includes desaturated colors, decreasing spatial details and a shift to blue hues. However, a painting, print or display cannot reproduce scotopic conditions for technical reasons and adaptation to such conditions would require long time. To nonetheless convey a

Author's address: P. Kellnhofer; e-mail: pkellnho@mpi-inf.mpg.de.

DOI 10.1145/2644813 http://doi.acm.org/10.1145/2644813

nocturnal mood, artists have employed several tricks to reproduce a nightly impression in painting [Livingstone 2002, Ch. 3] and since its early days in movie making where it is known as the "day-for-night" effect or the "American night". Several tricks are used to overcome the difficulty that an observer should feel as if at scotopic conditions but at the same time limiting the degrading effect of scotopic vision: an overly blurry and colorless image would not be useful (e. g., in an interactive application such as a game) and therefore not preferable. Consequently, everything that can make an image feel more scotopic without degrading it to become useless is highly desirable.

The physiological processes explaining the phenomena of scotopic perception are well understood [Hess et al. 1990]: the loss of color perception and acuity are due to the change from cone to rod vision while the increased sensitivity towards the shorter wavelengths in the visible color spectrum is known as the Purkinje shift. In computer graphics, physiological models were used to simulate how a scene would be perceived at night, including the course of adaptation [Ferwerda et al. 1996; Pattanaik et al. 2000; Durand and Dorsey 2000; Haro et al. 2006] and color shift [Thompson et al. 2002; Kirk et al. 2011]. Day-for-night tone mapping is a common effect in interactive computer applications such as games, where it is sometimes even a part of the gameplay (e. g., stealth action). In general, reproducing the appearance of one illumination setting using a medium that requires different conditions is a special form of tone mapping [Reinhard et al. 2010].

With the advent of stereoscopic reproduction, the question arises if and how depth perception changes in scotopic conditions and if so, how to account for it, both theoretically by a predictive perceptual model and in practical applications such as tone mapping. If monocular day-to-night tone mapping needs to reduce acuity and shift desaturated colors towards blue in images presented at photopic conditions, how do we need to change a stereo image presented at photopic conditions to most faithfully reproduce scotopic appearance? We address this question by two contributions:

—Measurement of disparity sensitivity in scotopic conditions

—A combined color-disparity manipulation approach to reproduce scotopic stereo appearance

2. BACKGROUND

Scotopic, mesopic, and photopic vision. Human vision operates in a wide range of luminance values (10^{-6} to $10^{8}\,\mathrm{cd/m^2}$) where rod photoreceptors are active in dark conditions up to about $3\,\mathrm{cd/m^2}$ while cone photoreceptors become sensitive for luminance above $0.1\,\mathrm{cd/m^2}$. Purely rod- and cone-mediated vision is called *scotopic* and *photopic* respectively; the range of mixed cone and rod activity is called *mesopic*.

The rod and cone responses are modeled in many applications, such as image quality metrics [Mantiuk et al. 2011], color appearance models [Kuang et al. 2007], and tone mapping operators [Ferwerda et al. 1996; Durand and Dorsey 2000; Ward et al. 1997]. In mesopic conditions, a linear combination of rod and cone response is typically considered. A biologically-inspired model that predicts the offset in the L, M, and S cones due to rod responses has been used in tone mapping [Kirk et al. 2011]. Our technique of disparity[1] adjustment for scotopic conditions can be combined with common tone mapping.

Stereoacuity in scotopic conditions. In a vast majority of graphics techniques dealing with stereo vision and binocular disparity processing, photopic vision is tacitly assumed [Lang et al. 2010; Didyk et al. 2011]. Lit [1959] reports an almost 20-fold disparity threshold increase in scotopic conditions with respect to photopic ones. While the threshold steadily increases across mid-photopic and mesopic conditions with decreasing adaptation luminance, at the transition between

[1] In this work we refer to the "disparity" of a point as the difference of the vergence angle for that point and a reference point, measured in arcminutes. The vergence angle of a point is measured between the optical axes of both eyes when verging on a point. By "pixel disparity" we denote the lateral distance in pixels between corresponding points in the left and right eye image. Pixel disparity is often a product of stereo-matching algorithms in computer vision and can be converted into vergence angles if the interocular distance and the display's distance, size and resolution are known.

mesopic and scotopic vision (where cones become inactive) a clear discontinuity in stereoacuity can be observed [Lit 1959; Lit and Hamm 1966]. Disparity estimation in the human visual system (HVS) is similar to windowed cross-correlation [Cormack et al. 1991; Filippini and Banks 2009], which is commonly used in computer vision. In this respect the difficulties in finding window correspondence for night photographs [Subr et al. 2012], can serve as an indicator of possible problems that the HVS might experience in dark conditions. Such problems include the reduced quality of eye optics due to a larger pupil size, more blur due to loss of central cone vision in the fovea and reduced acuity of peripheral rod vision, as well as neural circuitry and photon noise [Hess et al. 1990].

In our further discussion we focus on scotopic stereoacuity dependence on spatial frequencies and luminance contrast in the image, as well as issues of the comfortable disparity range.

Spatial frequency content. Banks et al. [2004] have investigated random dot stereograms of various density and they showed that spatial stereoresolution is limited by the Nyquist sampling limit at low dot densities and the spatial frequency of luminance patterns at high densities. Moreover, stereoresolution deteriorates with increasing retinal eccentricity, which is not attributable to a binocular vision deficit in the periphery, but rather the increasing size of receptive fields and low-pass filtering in the eye optics. Livingstone and Hubel [1994] have investigated line stereograms and noticed that in scotopic conditions stereoacuity is more reduced than Vernier acuity for relative line position, which are both examples of hyperacuity. This may suggest that cortical averaging mechanisms associated with hyperacuity are more complicated in the case of stereo vision and more sensitive for the poorer quality of rod input, where higher spatial frequency patterns are strongly suppressed [Shlaer 1937].

Luminance contrast. As discussed by Legge and Gu [1989] and Heckmann and Schor [1989], binocular disparity sensitivity strongly depends on the magnitude of luminance contrast. Didyk et al. [2012] considered this effect in the context of disparity manipulation using a stereoacuity model proposed by Cormack et al. [1991]. The model has been derived based on measurements for narrow-band-filtered random dot stereograms, and predicts an over tenfold disparity threshold increase for luminance contrast change from suprathreshold (over 10 just-noticeable-differences (JND)) to near threshold levels (2 JNDs). Since the model has been obtained through averaging the results for randomly chosen photopic and upper range mesopic luminance levels akin to a CRT display, the model validity for scotopic conditions is to be questioned. In this work, we investigate this issue. Since the sensitivity to luminance contrast is more than tenfold reduced for the change of adaptation luminance from photopic to scotopic conditions [Wandell 1995, Fig. 7.21], our goal is to model the resulting reduction of stereoacuity.

Disparity range. Another interesting finding on scotopic stereoacuity is a fourfold enlargement of Panum's area of binocular fusion with respect to photopic conditions. This is well beyond fusion limits that can be predicted from the well-known spatial frequency and contrast effects [O'Shea et al. 1994]. This means that for night scenes reproduced on high dynamic range (HDR) displays, disparity compression, which is often performed to reduce visual discomfort, can be relaxed. This does not apply to low dynamic range (LDR) displays, which are considered in this work, as the viewer luminance adaptation is mostly at photopic levels.

3. OVERVIEW

Our approach emulates the appearance of scotopic stereo on a photopic stereo display. As illustrated in Fig. 1, stereoacuity is lower in scotopic conditions. Consequently, day-for-night stereo has to degrade the stereo content to match the scotopic experience. To this end we address two questions: how does stereoacuity behave in scotopic conditions and how do we need to process disparity to account for it?

To address the first question, we conduct a series of experiments to relate adaptation luminance to threshold elevation in the discrimination of binocular disparity patterns (Sec. 4). This experiment complements the findings of Cormack et al.

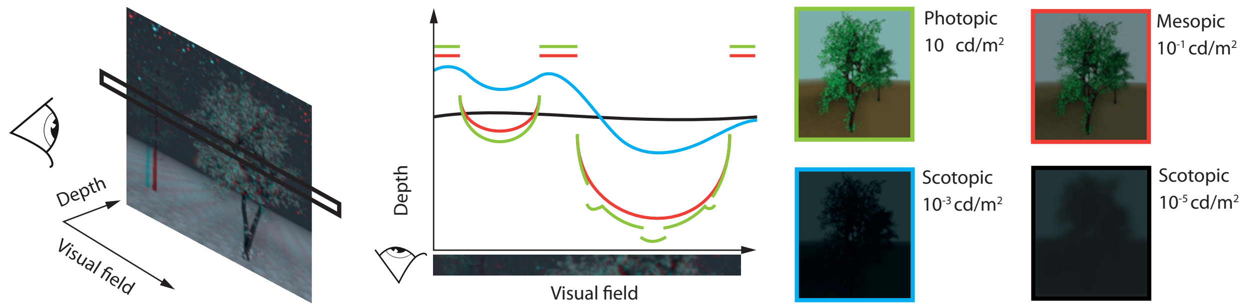

Fig. 1. A one-dimensional cross section (horizontal axis) through the perceived depth (vertical axis) of a stereo rendering of trees such as the one in Fig. 8 for different adaptation states (colors). Under photopic conditions, all stereo details such as leaves are visible and the trees are fully separated. In mesopic conditions, stereo details start to disappear and the range gets smaller. Under scotopic conditions, only rough structures remain, that disappear before the luminance is too low to perceive an image entirely.

[1991], who measure the relation of luminance contrast and disparity perception for mostly photopic conditions. In pilot experiments, we identify a well-discernible pattern that limits monocular stereo cues, as well as each participant's individual luminance contrast detection thresholds. A final experiment is conducted by presenting stereo stimuli in different adaptation conditions that range over eight orders of magnitude using an HDR stereo display in combination with neutral density optical filters.

Addressing the second question, we describe how to process disparity to produce a scotopic stereo impression (Sec. 6). We use the result of the perceptual experiment to identify stereo details that would not be perceived if the scene actually was scotopic and remove them. The processing is conceptually simple and can be computed at interactive frame rates.

4. PSYCHOPHYSICAL EXPERIMENTS

We repeat the experimental procedure of Cormack et al. [1991] to find how the luminance contrast and disparity detection thresholds change in scotopic conditions, which have not been studied so far. Even existing monocular contrast perception models [Mantiuk et al. 2006] differ significantly with respect to sensitivity measurements under different levels of adaptation luminance.

We perform three experiments. The first two are pilot experiments to establish a reliable monocular baseline which is required for two reasons. First, it is not obvious which luminance pattern to use, so we test several alternatives (Sec. 4.2). Second, luminance contrast detection thresholds vary between observers and need to be known to model the effect in a longitudinal study with the same observers under different conditions (Sec. 4.3). Finally, the third experiment quantifies the relation of luminance adaptation and disparity detection thresholds (Sec. 4.4) and produces the model actually required to perform stereo day-for-night conversion (Sec. 5).

4.1 Methods

Stimuli. The stimuli are random square stereograms (RSSs) composed of a regular grid of randomly black or white squares with equal probability on a gray background (Fig. 2b). To create the desired luminance contrast, we ensure equal brightness steps between the black, gray, and white levels used, thereby matching the average brightness of the stimuli to the background. The gray background luminance is also the adaptation luminance.

The stimuli have horizontal depth corrugations in the form of a square wave created by 8 equally spaced steps in disparity that coincide with some of the horizontal luminance edges between two rows of squares. The luminance

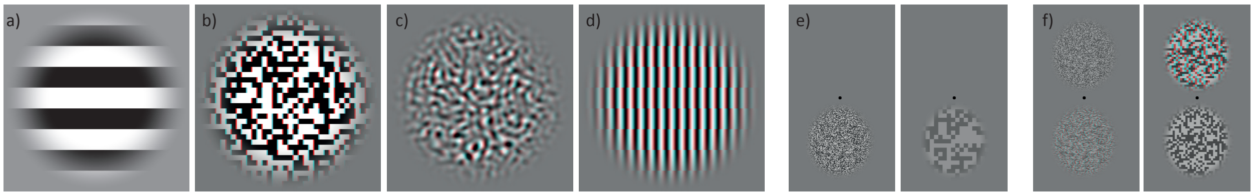

Fig. 2. (a) Depth map used in all experiment stimuli. (b) Example random square stereogram (RSS) stimulus. Alternative stimuli such as (c) bandlimited noise or (d) sine wave gratings were rejected because of false monocular cues to disparity. Screen layout used in Experiments 1 and 2 (e), and Experiment 3 (f) optimized for various adaptation levels.

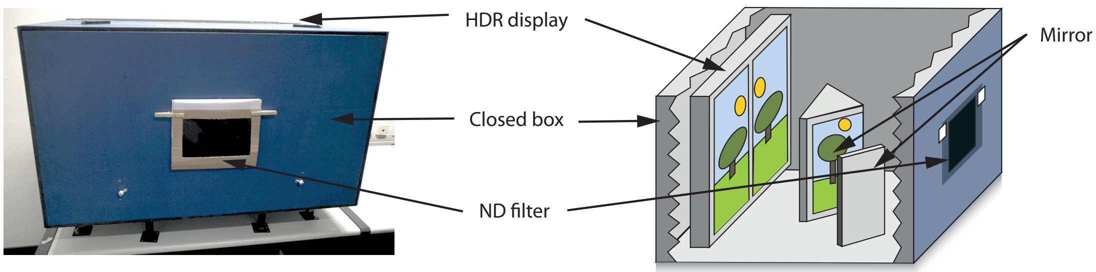

Fig. 3. Wheatstone HDR stereoscope and filter aperture.

contrast is faded out smoothly at the edge of the stimuli to avoid monocular cues due to the disparity shift. The average depth of the stimuli is at the screen plane to avoid vergence-accommodation conflicts.

RSS stimuli were chosen to resemble the stimuli used by Cormack [1991] but at varying, coarser resolutions to account for scotopic conditions. Several alternative luminance patterns were considered, including band-limited noise, Gabor patches, and sine-wave gratings (Fig. 2c,d), but as they do not allow alignment of the disparity edges with existing luminance edges, and instead each disparity edge creates a new luminance edge, this would result in a monocular depth cue.

Apparatus. Stimuli are presented on a 47" SIM2 HDR47E high dynamic range display with 1920×1080 resolution. Each half of the screen is directed to one eye by a Wheatstone [1838] stereoscope enclosed in a black box with a small viewing aperture to avoid any stray light (see Fig. 3). The viewing distance to the screen is 90 cm, giving each pixel a size of approximately 2 arcmin. This display system is set up in a dark room and was radiometrically calibrated to accurately and reliably produce any luminance value between 1 and 1000 cd / m^2. Rosco E-Colour+ neutral density filters with specified optical densities of 0 (no filter), 1.2, 2.4, 3.6, or 4.5 cover the viewing aperture to produce the required scotopic luminances while preserving the displayed luminance contrast. Our own measurements confirmed that the transmittance of the filters was within 4.5 % of the specifications.

Procedure. All thresholds are estimated with two-alternative forced-choice (2AFC) adaptive staircase designs using QUEST [Watson and Pelli 1983]. Stimuli are presented simultaneously in two locations, above and below a black fixation dot at the center of the screen (Fig. 2e,f). Between trials the screen is blanked to a slightly darker gray level than the gray background used during trials. The staircases are repeated several times and the results of the converged staircases are averaged.

Observers. 3 observers participated in the experiments: 2 authors (B and C) and 1 experienced psychophysical observer (A) who was naïve regarding the purpose of the experiment, all male, age 24–31 ($M = 27$, $SD = 3.6$). Participants had normal or corrected-to-normal visual acuity and did not have stereo-blindness or night-blindness. We find 3 observers sufficient as the time needed for complete measurement consisting of many staircases is in the order of several hours and the variance between observers is low. A small number of participants in complex psychophysiological experiments is also common in comparable studies [Cormack et al. 1991; Livingstone and Hubel 1994] that measure similar phenomena.

4.2 Optimal RSS Frequency Selection (Exp. 1)

The first experiment is conducted in monocular conditions and identifies the best luminance pattern frequency for each luminance adaptation. The frequency is defined by the inverse of the size of the squares. In this experiment, a stimulus with luminance contrast between 0 and 1 Michelson units is presented in either the top or bottom location. The other location remains blank. There are no depth corrugations in the RSS stimuli, i. e., all squares are presented at screen depth.

The luminance contrast detection thresholds are estimated at each square size (2, 4, 8, 16, or 32 pixels, or 4, 8, 16, 32, or 64 arcmin) and adaptation luminance level (10, 0.631, 0.04, 0.003, or 0.0003 cd / m^2) by averaging the results of 2 staircases. The lowest threshold occurs for the optimal square size for each adaptation luminance level. The optimal square sizes (2, 8, 8, 16, and 32 pixels) are used in the following experiments in their respective adaptation luminance level.

A single observer (B) determined the optimal size of the squares in the RSS stimuli, which leads to highest sensitivity to luminance contrast detection for each adaptation luminance. Note that we repeat the experiment of Cormack et al. over a wide range of adaptation luminances, where the peak of contrast sensitivity shifts towards lower spatial frequencies with decreasing luminance [Wandell 1995, Fig. 7.21]. Since our extension of the function measured by Cormack et al. will be parametrized by adaptation luminance, and specifies stereoacuity thresholds as a function of contrast scaled in JND units, the goal of this experiment is to derive RSS stimuli that lead to conservative (as small as possible) contrast detection thresholds. This way a common basis in deriving the Cormack function is established, which enables its meaningful interpretation across all lighting conditions.

While the contrast sensitivity function (CSF) might already predict the optimal visible frequency, we decided to perform this calibration experiment, as our stimuli do not consist of sinusoidal gratings of a single frequency with which the CSF was measured (the reason is recalled in Fig. 2) but of boxes which combine all frequencies in a way that is complex to model.

4.3 Luminance Contrast Detection Threshold (Exp. 2)

The same experiment as before is now performed by all observers, using only the optimal spatial frequency of the RSS squares for each adaptation luminance, to determine their luminance contrast detection thresholds by averaging the results of 3 staircases. These thresholds (see Fig. 4) will be used as the JND units of luminance contrast in the following experiment.

4.4 Disparity Detection Threshold (Exp. 3)

In this experiment, a stimulus is presented in either the top or bottom location with disparity between 0 and 30 arcmin at the depth corrugation edges, which corresponds to 18 cm between the near and far parts of the corrugation. Disparities up to 30 arcmin were included to provide sufficient operational space to the staircase, in particular at the lowest adaptation luminance level. Such horizontal disparity is still within the fusion range[Qin et al. 2006]. No convergence to disparity thresholds higher than 15 arcmin was observed in practice. A stimulus with the same luminance pattern but without any depth corrugations is presented in the other location. The disparity detection thresholds are estimated by averaging the results of 2 staircases at the same adaptation luminance levels as before and at 4 luminance contrast levels starting at 2 or 3 JNDs (as measured in the previous experiment) and increasing logarithmically to the maximum verified contrast of the display (see Fig. 5). Stimuli at luminance contrast levels below 2 JNDs are not sufficiently visible to allow disparity detection. The optimal spatial frequency of the RSS squares is used for each adaptation luminance.

5. MODEL

We will now fit the result of the previous three experiments to a closed-form model of luminance contrast sensitivity and disparity sensitivity.

Luminance contrast sensitivity model. First, the results of the contrast detection threshold experiment for all observers are fit to a power function that maps from adaptation luminance L_a to mean luminance contrast detection threshold C_Thr

$$C_\mathrm{Thr}(L_\mathrm{a}) = c_1 {L_\mathrm{a}}^{c_2},$$

where $c_1 = 0.0145$ and $c_2 = -0.314$ (Fig. 4; Degree of freedom-adjusted $R^2 = .94$). Note that this function resembles the well-known contrast versus intensity-functions (c. v. i.) [Reinhard et al. 2010, Sec. 10.7.2], here expressed in threshold magnitudes which are inversely proportional to the typically plotted sensitivity. We measure our thresholds for luminance RSS patterns that are directly used for the stereoacuity measurements in Exp. 3. Using threshold C_Thr, luminance contrast $C_\mathrm{JND}(C_\mathrm{M}, L_\mathrm{a}) = C_\mathrm{M}/C_\mathrm{Thr}(L_\mathrm{a})$ (expressed in JND units) is computed for the luminance adaptation L_a and Michelson contrast C_M following the procedure of Cormack et al. [1991].

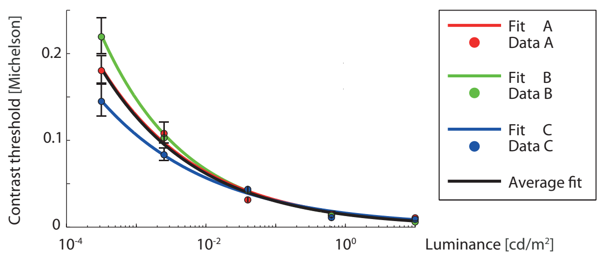

Fig. 4. Mapping from adaptation luminance L_a to luminance contrast detection threshold C_Thr fitted from Exp. 2 in Sec. 4.3.

Disparity sensitivity model. Next, we compute the disparity threshold D for adaptation luminance L_a and luminance contrast C_JND. We provide both a non-linear and a linear fit to the measurements from Exp. 3. The non-linear model is

$$\log_{10} D_\mathrm{nl}(L_\mathrm{a}, C_\mathrm{JND}) = \frac{c_3}{\log_{10} C_\mathrm{JND} + c_4} \cdot ({L_a}^{c_5} + c_6),$$

where $c_3 = 0.485$, $c_4 = 0.893$, $c_5 = -0.181$, $c_6 = 5.21$. A fit of each separate observer and a combination of all observers is shown in Fig. 5, bottom (Degree of freedom-adjusted $R^2 = .77$ for combined observers; $R^2 = .83$, .95, and .95 for individual observers). The nonlinear model saturates thresholds for suprathreshold contrast and adaptation luminance levels. An alternative linear fit is

$$\log_{10} D_\mathrm{lin}(L_\mathrm{a}, C_\mathrm{JND}) = c_7 \log_{10} C_\mathrm{JND} + c_8 \log_{10} L_a + c_9,$$

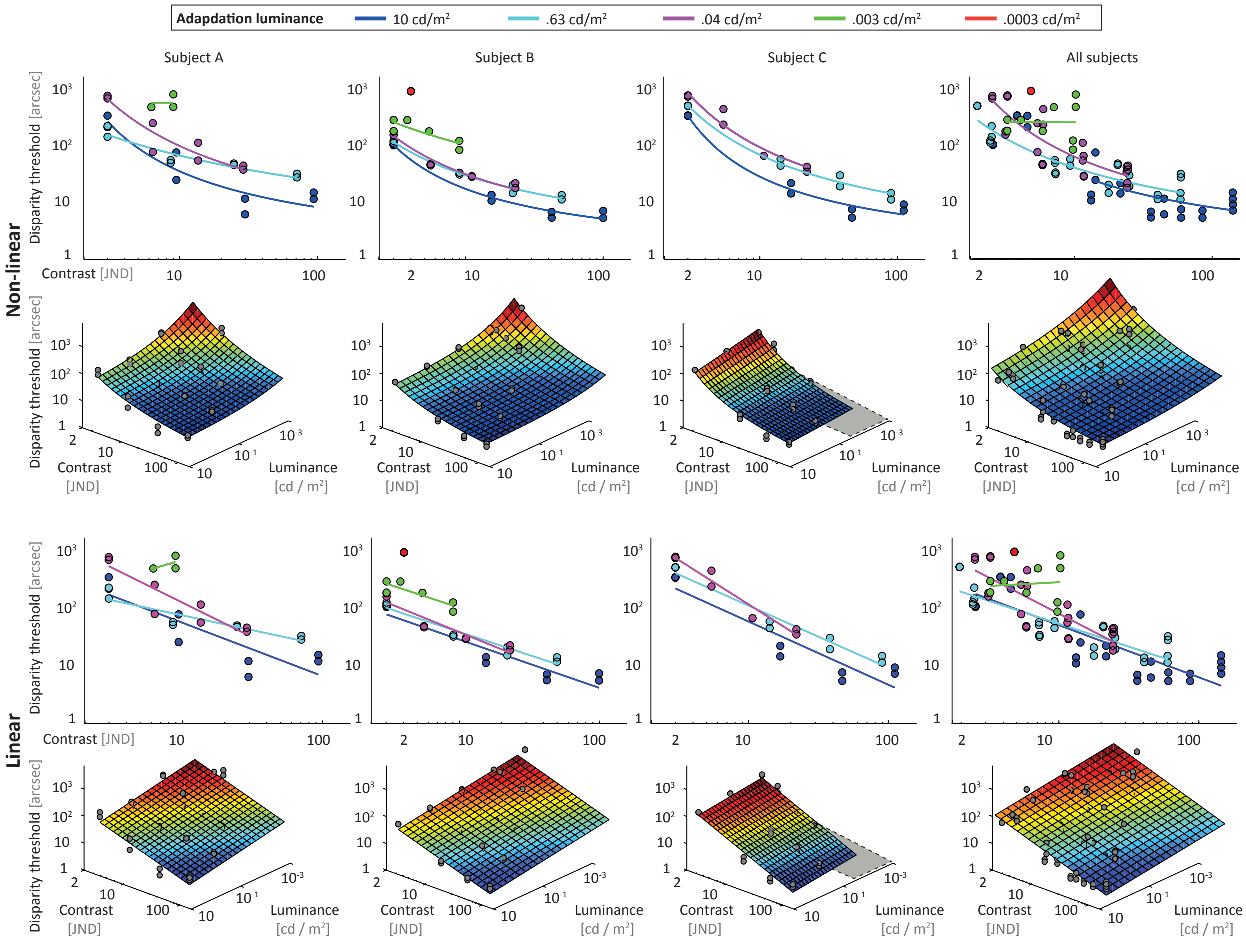

Fig. 5. Mapping from luminance contrast C_{JND} and adaptation luminance L_{a} to disparity threshold D fitted to Exp. 3 by a non-linear and a linear function in Sec. 4.4.

where $c_7 = -0.873$, $c_8 = -0.155$, $c_9 = 2.618$. A fit of each separate observer and a combination of all observers is shown in Fig. 5, top (Degree of freedom-adjusted $R^2 = .75$ for combined observers; $R^2 = .78$, $.88$, and $.91$ for individual observers).

The linear model is simpler and computationally more effective, but provides a lower quality-of-fit in terms of R^2 as it lacks the saturation the non-linear model provides. We did not observe a large influence of model choice on our end results and use the non-linear model $D(L_{\text{a}}, C_{\text{JND}}) = D_{\text{nl}}(L_{\text{a}}, C_{\text{JND}})$ in the following.

Discussion. We find that the difference of our scotopic disparity thresholds to the photopic ones is up to 20-fold and on average 12-fold depending on contrast. Such large differences are commonly visualized in logarithmic space (see Fig. 5). We applied logarithmic scaling to the adaptation luminance to get closer to the non-linear sensitivity of the HVS and also to keep plots comparable with those of Cormack et al. [1991]. We chose the functions $D(L_{\text{a}}, C_{\text{JND}})$ to model the influence of luminance contrast and adaptation luminance as two independent effects. We performed the least-square fitting in the same logarithmic-logarithmic space to achieve perceptually meaningful fitting errors. As a result, logarithms are present in both alternatives for $D(L_\mathrm{a}, C_\mathrm{JND})$. In case of non-linear fit it further increases the apparently complicated form of the model, otherwise consisting of a simple mix of rational and exponential function. The logarithm applied to the function C_JND was removed by substitution $z^{a \cdot \log_z x} \equiv x^a; z \in \mathbb{R}^+$ turning the exponential function into a power function.

Our photopic disparity thresholds are on average fourfold higher than those reported for similar contrast JNDs by Cormack et al. [1991]. This can be caused by the different procedure used to scale contrast in JNDs or by differences in the disparity threshold measurements themselves. Absolute threshold magnitudes cannot be compared between publications, but relative differences inside a single experiment likely remain valid. Therefore, our contrast-disparity threshold function has a similar shape as the one of Cormack et al. [1991].

6. STEREO CONTENT PROCESSING

In this section, we show how to process stereo content to match luminance adaptation, i. e., to produce a scotopic appearance on a photopic stereo display. The goal is to achieve visually plausible stereoscopic image reproduction by reducing the acuity of disparity perception in a similar way as during true scotopic adaptation. This consequently also decreases the performance for tasks requiring depth understanding or object segmentation, e. g., spotting an enemy in a computer game. To this end, we will change both the disparity (Sec. 6.1), and the luminance (Sec. 6.2). The input to our stereo day-for-night conversion is stereo content captured at photopic conditions and a desired new luminance adaptation condition. The output is stereo content that resembles a scotopic stereo impression when shown in photopic conditions. We process stereo content in the form of an image pair, in combination with a per-pixel vergence map. Every pixel of this map stores the angle the eyes would form when verging to it. Such a vergence map can be computed from the interocular distance and the screen's distance, size and resolution, in combination with the pixel disparity that is readily output by interactive applications such as computer games, as well as by movie production, and can be approximated from a stereo pair using computer vision approaches.

Some pixels are only visible in one image of the stereo image pair (occlusions). As they cannot be matched with a pixel in the other image of the pair, they require special consideration. For computer-generated content, the depth at such pixels is known. For computer-vision content, filling such pixels with plausible depth values is up to the stereo reconstruction used. Therefore, in both cases, vergence can be computed for every pixel, even if occluded in the other image. The resulting maps are identical in unoccluded regions but differ in occluded regions. While this is not perceptually principled, it allows for a practical solution in which the pipeline is executed twice, with a different vergence map for each image of the stereo pair.

6.1 Disparity Processing

Disparity processing first filters the vergence map and then warps both images in the stereo image pair to match the filtered result. We will first list the requirements of this processing and give some necessary definitions, before explaining the process itself.

Requirements. The input vergence map should change such that disparity that would be perceived weaker or not at all in scotopic conditions is weakened or removed entirely. First, all combinations of physical disparity with luminance contrast below 1 JND in scotopic conditions – and therefore imperceptible – are removed. In particular, fine details with low luminance contrast will disappear [Frisby and Mayhew 1978]. Second, the overall range of disparities will be reduced: While photopic conditions reproduce a wide range of disparity JNDs, in scotopic conditions this range is arbitrarily low, up to the point where luminance patterns are still discernible, but no stereo perception is present.

One could argue that changing the photopic image luminance to emulate scotopic conditions is sufficient to already degrade the stereo perception to meet those requirements. The existence of day-for-night techniques demonstrates that this does not apply in practice: displays are not capable of producing scotopic image conditions, the viewing conditions do not allow for adaptation, and even if they could, adaptation would take a considerable time. Finally, directly changing luminance to produce a scotopic depth perception (reduced contrast, blur) would lead to severe degradation of the image and render the content unusable as seen in Fig. 6. Consequently, even if color image day-for-night reduces

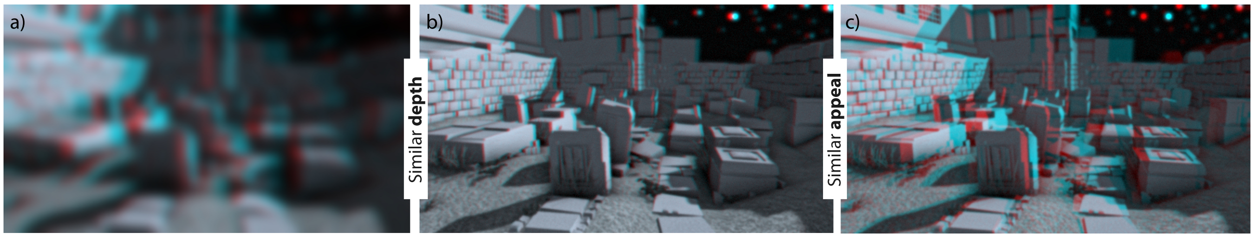

Fig. 6. *a):* Directly simulating scotopic vision by degrading luminance results in the desired reduced depth, but produces an overly blurry image that lacks contrast and consequently has become useless in practice. *b):* Our approach matches the disparity to be similar to scotopic depth perception in combination with luminance that was created using common day-for-night *(c)*, producing results that both have correct depth and visual appeal.

the luminance to the low end of the range afforded by the display device, it has to remain photopic and so does its stereo perception. Emulating the image hue and saturation degradation due to scotopic conditions could reduce stereo perception to some extent [Simmons and Kingdom 1997; 2002]. However, common day-for-night luminance, hue, and saturation processing applied to stereo pairs does not match the reduced stereo perception of real scotopic conditions (see Fig. 8). We conclude that disparity itself needs to be altered in order to produce scotopic stereo appearance.

Notation. We denote the input and output vergence maps as $d_{\mathrm{in}} \in \mathbb{R}^2 \to \mathbb{R}$ and $d_{\mathrm{out}} \in \mathbb{R}^2 \to \mathbb{R}$. Further, we denote the input and output RGB images as $I^{\mathrm{In}} \in \mathbb{R}^2 \to \mathbb{R}^3$ and I^{Out}. The color image processing is performed twice: once for I^{In} from the left and once from the right eye's view. The disparity processing for d_{in} is performed once and applied to both color images. Finally, the adaptation luminance we would like to emulate is denoted as $L_{\mathrm{a}}^{\mathrm{In}}$, typically ranging from 10^{-4} cd / m^2 to 10^{-1} cd / m^2 and the current display condition adaptation $L_{\mathrm{a}}^{\mathrm{Out}}$ between 1 and 100 cd / m^2.

Disparity processing. First, the Michelson luminance contrast C_{M} (Fig. 7e) is computed from a Laplacian pyramid [Burt and Adelson 1983] of a luminance image (Fig. 7c) which has been mapped for target scotopic luminance $L_{\mathrm{a}}^{\mathrm{Out}}$ by filtering the luminance with the CSF cutoff (Fig. 7d). The highest spatial frequency of luminance resolvable by the HVS was determined using the acuity function (Eq. 15 from Ward et al. [1997]). This possibly very blurry image (Fig. 7d) is never actually shown to the user, but only serves as a proxy to predict stereo perception. That allows separate processing of luminance and disparity, and therefore achieves both artistic goals in the luminance domain and physiologically correct presentation in the disparity domain.

Next, the vergence map d_{in} (Fig. 7b) is decomposed into another Laplacian pyramid (Fig. 7f), which effectively contains differences of vergence angles, i. e., disparity δ. Note that both pyramids are fully analogous, which means that the corresponding value of luminance contrast C_{M} can be immediately found for any spatial frequency band and spatial location where the disparity δ is defined. This is important as our goal is to reduce the disparity perception in the scotopic luminance adaptation $L_{\mathrm{a}}^{\mathrm{In}}$ with respect to the photopic condition adaptation $L_{\mathrm{a}}^{\mathrm{Out}}$ given the luminance contrast C_{M}. To perform such a reduction in a visually meaningful way we need to transform the physical disparity magnitude δ into a perceptually linear sensory response space, where the linearized disparity values δ^* better correspond to actually perceived depth changes. (A direct analogy to the CIE L*a*b* color space, where differences are proportional to perceived differences.) The transducer functions $\delta^* = t(\delta)$ serve this purpose [Didyk et al. 2011] by taking into account

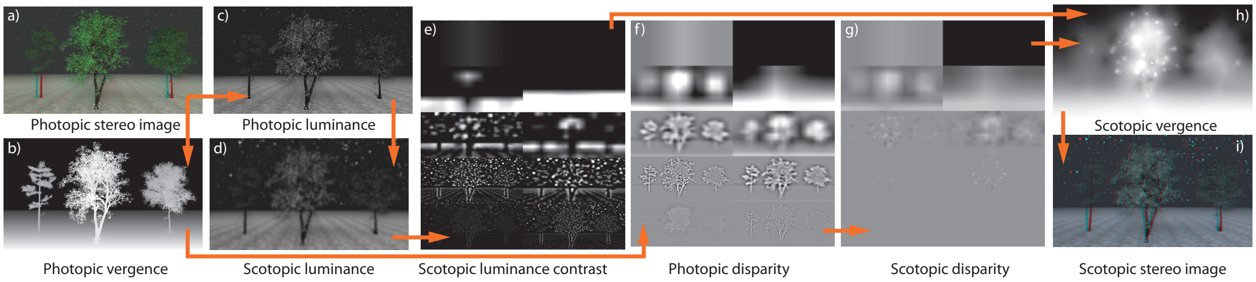

Fig. 7. Disparity processing steps (orange arrows) in our pipeline explained in Sec. 6: *a, i):* Input and output HDR stereo image in physical units shown in anaglyph. *b, h):* Input and output vergence (visualized as gray). *c, d):* Photopic and scotopic luminance. *e)*: All bands of the luminance contrast pyramid (decreasing frequency from bottom-left to top-right; brighter is more contrast). *f, g):* Photopic and scotopic disparity (Laplacian of vergence); same layout; black indicates negative, gray neutral and white positive disparity.

the increase of disparity discrimination thresholds with increasing pedestal disparity. Due to the compressive nature of the disparity transducer it can be approximated by a simple logarithmic function $\delta^* = 21\log_{10}(\delta + 0.82)$, which is a fit to the data in [Didyk et al. 2011, Fig. 3.6] for depth corrugations of spatial frequency of 0.3 cpd, where the HVS sensitivity is the highest. We employ this transducer to transform all values in the disparity magnitude pyramid. Since the transduced disparity δ^* models the hypothetical response of the HVS, one can perform linear operations on its values so that the scaling $s \cdot \delta^*$ translates directly into the perceived depth reduction. We define such a scaling as a ratio of perceptually linearized disparity sensitivities $D^* = 21\log_{10}(D(L_\mathrm{a}, C_\mathrm{JND}) + 0.82)$ for the photopic and scotopic adaptation luminance $L_\mathrm{a}^\mathrm{Out}$ and L_a^In:

$$s(C_\mathrm{M}, L_\mathrm{a}^\mathrm{In}, L_\mathrm{a}^\mathrm{Out}) = \frac{\log\left(D(L_\mathrm{a}^\mathrm{Out}, C_\mathrm{JND}(C_\mathrm{M}, L_\mathrm{a}^\mathrm{Out})) + 0.82\right)}{\log\left(D(L_\mathrm{a}^\mathrm{In}, C_\mathrm{JND}(C_\mathrm{M}, L_\mathrm{a}^\mathrm{In})) + 0.82\right)},$$

for suprathreshold of $C_\mathrm{JND}(C_\mathrm{M}, L_\mathrm{a}^\mathrm{In}) \geq 2$ JND, as

$$s(C_\mathrm{M}, L_\mathrm{a}^\mathrm{In}, L_\mathrm{a}^\mathrm{Out}) = 0$$

for $C_\mathrm{JND}(C_\mathrm{M}, L_\mathrm{a}^\mathrm{In}) \leq 1$ JND and as a smooth ramp between the two on the interval from 1 to 2 JND. The special treatment of luminance contrast below 1 JND was chosen to avoid extrapolation out of the range of our measurements. It models the absence of disparity perception in low contrast regions [Frisby and Mayhew 1978]. The luminance contrast on a given frequency band is defined as the maximum contrast in the sub-pyramid corresponding to equal or higher frequencies [Didyk et al. 2012]. To predict the effect of luminance contrast on disparity, each prior transduced disparity band is multiplied by $s(C_\mathrm{M}, L_\mathrm{a}^\mathrm{In}, L_\mathrm{a}^\mathrm{Out})$ (Fig. 7g). As usually $s(C_\mathrm{M}, L_\mathrm{a}^\mathrm{In}, L_\mathrm{a}^\mathrm{Out}) < 1$, disparity is effectively compressed, when displaying scotopic luminance on a photopic display ($L_\mathrm{a}^\mathrm{In} < L_\mathrm{a}^\mathrm{Out}$).

Finally, the inverse photopic transduction (a simple exponential function is used in this work to invert the logarithmic transducer) converts perceived disparity δ^* back to physical disparity δ [Didyk et al. 2011] and the scotopic vergence map is reconstructed using the inverse Laplacian transform (Fig. 7h).

Despite the involved perceptualization steps, the entire disparity processing can be efficiently performed on a GPU in a time linear in the number of pixels. Our implementation processes a single Full HD vergence map (1920×1080) in 18 ms on an Nvidia Quadro 4000.

Discussion. Note that although the resulting dynamic range compression of perceived depth under scotopic conditions clearly is a suprathreshold effect, the luminance contrast-dependent ratio $s()$ of perceivable disparity thresholds in photopic and scotopic conditions is used for this manipulation. Patel et al. [2009] observe that in the presence of blur not only the stereoscopic disparity thresholds are increased, but also the perceived suprathreshold stereoscopic depth is reduced. They attempt to explain their data on the perceived depth reduction using various sensory-perception transducer functions, including the logarithmic compression employed in our work, in which case the gain factor must be reduced. Note that the gain factor directly corresponds to our scaling $s()$, which we use for modeling both the perceived depth reduction and disparity detail suppression in scotopic conditions as a function of local luminance contrast. Unfortunately, only +2D of dioptric blur was considered by Patel et al. , while presenting high contrast bright lines of $30\,\mathrm{cd}\,/\,\mathrm{m}^2$ that are imposed on a dark background, which makes those data too limited for our purposes. Clearly, further research is needed to investigate the impact of suprathreshold disparity magnitudes on the value of the scaling factor $s()$, which in this work relies on the threshold data. Note that this would require collecting data in a 5D space (adaptation luminance, luminance contrast, luminance spatial frequency, disparity magnitude, disparity spatial frequency), while in this work we focused on the first three dimensions, which are the most relevant for typical day-for-night image manipulations.

Image pair warping. From the modified vergence map a stereoscopic image pair needs to be produced. First, the modified vergence is converted into modified pixel disparity assuming a fixed interocular distance, and display distance, size and resolution. The new image pair is created by warping, i. e., deforming the two images of the image pair such that features that had the original pixel disparity before processing, now produce the desired pixel disparity. This can be done in two ways: first, if the scene is sufficiently simple or the depth map is acquired from computer vision, depth image-based rendering (DIBR) [Fehn 2004] is used to produce a new image pair. Second, for rendered scenes, 3D geometry warping [Kellnhofer et al. 2013] achieves superior results, which do not suffer from disocclusions or sampling problems that are inherent for DIBR.

6.2 Luminance Processing

Both images of the stereo image pair are processed to simulate monocular scotopic vision phenomena such as loss of acuity, the Purkinje shift and noise using the method of Thompson et al. [2002]. We used equation 15 from Ward et al. [1997] for physiologically-based spatial acuity. The luminance processing requires 30 ms on the aforementioned Nvidia Quadro 4000.

7. RESULTS

Typical results of our approach are shown in Fig. 8. For each scene, the original photopic scene, the same scene with day-for-night tone mapping but the original stereo, and our combined luminance-stereo day-for-night are shown. Along with each scene, the original and modified disparity maps are shown as an inset.

The first row in Fig. 8 shows a virtual scene of a graveyard at night. After stereo day-for-night, small stereoscopic details, such as the vegetation in the foreground are removed, which remained visible in common day-for-night tone mapping. Also the overall depth range is reduced. Using our approach, the individual gravestones in the foreground are still separated, whereas the gravestones in the back – even if their physical distance is the same as in the foreground – do not produce a perceivable distance anymore. In common day-for-night, all gravestones are separated, which overestimates scotopic depth perception. The engravings in the stones and the structure of the back wall in the left have also disappeared after stereo day-for-night, even if they are still clearly perceived in the luminance image. This margin serves as an example for the fact that degrading the luminance alone is not sufficient to produce a scotopic stereo impression.

The second row in Fig. 8 shows a night driving stereo rendering. This shows a typical application, where simulation of scotopic stereo performance on a photopic screen is essential. A driving simulation requires real-time feedback, which is possible thanks to our GPU implementation. While the closer car to the left can still be discerned from its surrounding in depth, the remote car to the right has no remaining depth difference in respect to the other car. This

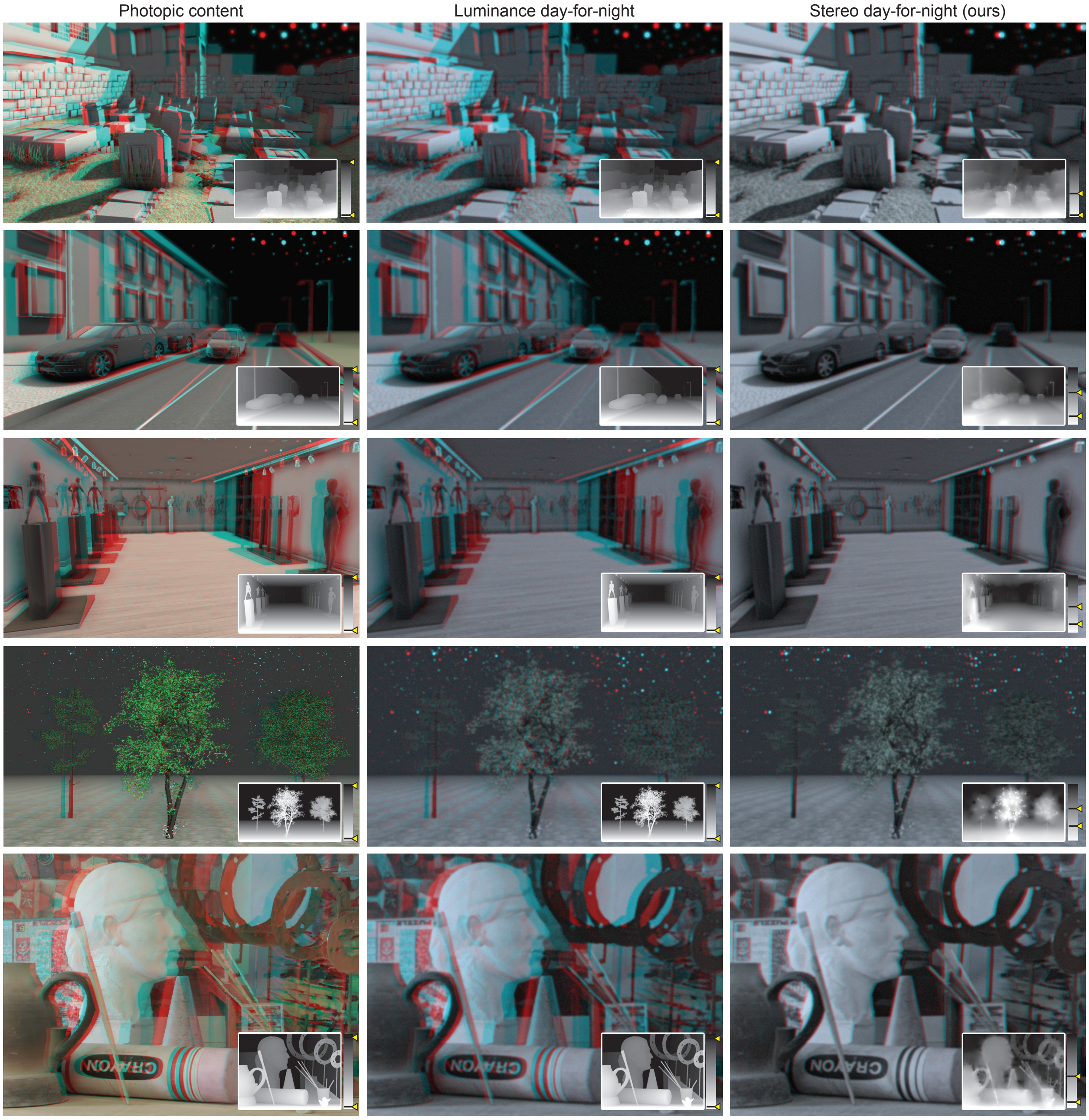

Fig. 8. Low-light stereo content *(rows)*, processed using: Original *(1st column)*, common day-for-night color tone mapping [Thompson et al. 2002] *(2nd column)*, our stereo day-for-night *(3rd column)*. Insets show the disparity with markers on the bar denoting the actual disparity range used. Common day-for-night tone mapping reproduces the desaturation, loss of acuity and blue shifts, but results in a mismatching depth impression, which is only perceived in photopic conditions. Our approach matches stereo fidelity to the actual scotopic percept. Captured stereo image *(5th row)* is courtesy of the Middlebury Stereo database [Scharstein and Pal 2007].

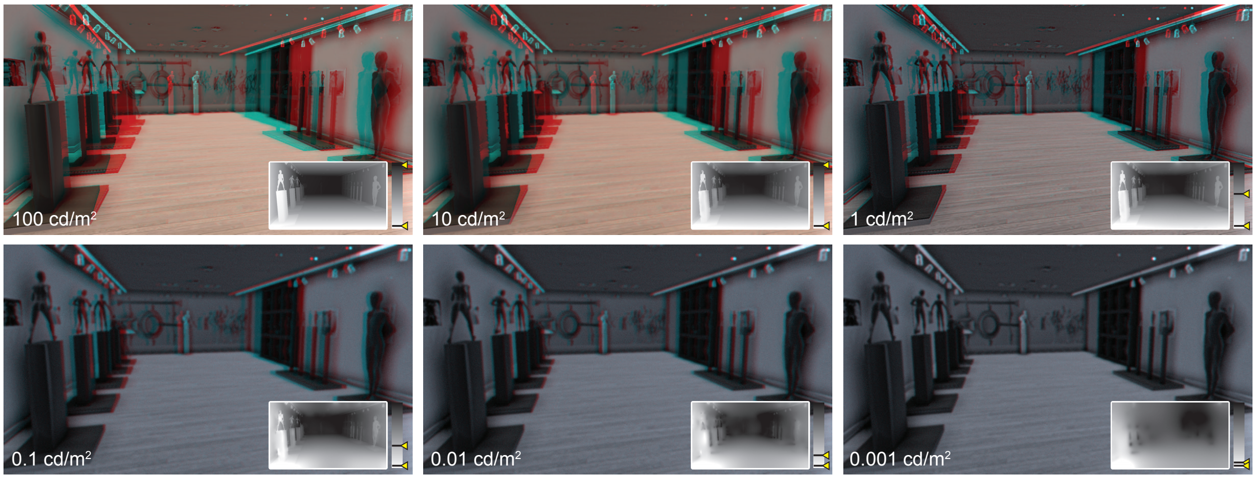

Fig. 9. Results of applying our stereo day-for-night to an architectural scene at six different adaptation luminance levels L_a^{In}. RGB tone mapping controlled independently and simulated for adaptation level not lower than $0.1 cd / m^2$ to prevent visual degradation.

effect is increased due to the fact that the car is both distant, has little contrast and has a low luminance. The third row in Fig. 8 shows an art gallery room. Dark indoor environments are another common situation inducing scotopic vision. Here the statues on the far right blend with the surrounding wall while larger statues in the front left are still differentiable. The fourth row shows a rendered landscape with trees. At night, the range is drastically reduced, but also small details disappear, which are still visible when only degrading luminance. The trees still do have a perceivable depth difference, but their depth details have disappeared. The fifth and final row shows a captured stereo image from the Middlebury Stereo database [Scharstein and Pal 2007]. Here, dark edges such as the rings or fine structure on the pencil have disappeared, that were still present in the luminance image after common day-for-night tone mapping.

In general all our results exhibit compression of small disparity gradients which corresponds to inability of an observer to distinguish small objects with low luminance contrast from the background. As a result of threshold elevation the absolute disparity range of all scenes is scaled down. One might argue that such scaling is not motivated by real world observations where perceived large scale distances do not change with illumination.

Given the large difference between scotopic and photopic disparity discrimination thresholds, many disparity gradients that are not observable at real scotopic conditions would become visible in photopic LDR display conditions. Using our scaling we detect such events and modify the disparity so that details that would be below 1 JND in scotopic conditions stay below 1 JND in photopic conditions. This ensures the preservation of detail visibility and invisibility. As a consequence, the total disparity range obtained by integrating such a disparity map is also rescaled. However, the 3D percept is maintained in areas where it would be expected, and the price of global depth range compression is typically acceptable to achieve the given objective. We also argue that in practice physically correct depth is rarely used as most scenes are usually larger than what the accommodation-vergence conflict would allow to present using current display technologies [Hoffman et al. 2008; Lambooij et al. 2009].

Our disparity mapping supports a large range of adaptation luminances (Fig. 9), where the luminance and disparity tone mapping could be controlled independently to achieve the desired artistic effect. This way the trade-off between perceptually correct depth detail preservation and physically correct depth range in the scene can be controlled.

8. USER FEEDBACK

Validating our model is particularly challenging: a simple preference study would merely confirm that viewers dislike visual impairment, not whether the model depicts night scenes more realistically. A true validation of this model would require a comparison of depth perception performance between real scotopic conditions and simulated darkness in photopic conditions. The time required to dark-adapt prevents any direct comparison. For this reason, we report only informal user feedback collected as follows:

We invited $N = 9$ observers to dark-adapt for 10 minutes and asked them to memorize the appearance of the Graveyard, Driving, and Art Gallery scenes from Fig. 8 in scotopic stereo conditions. Observers then adapted back to office lighting for one minute and were presented the same three scenes in photopic display conditions, using a classic day-for-night luminance-only tone mapping [Thompson et al. 2002] and our approach vertically next to each other for unlimited time.

Observers were asked to answer the following questions and give any additional comment they would like to make.

(1) Which image looks most similar to the scotopic image you saw?
(2) Which image looks more like realistic night vision?
(3) Which image would you prefer in a video game?

Interpreting the direct answers to our questions as 2AFC results in no significant effect (binomial test), except the following statement: The Graveyard scene with classic day-for-night is preferred and more similar to scotopic conditions (both $p < .02$). Observers also made the following comments:

—"Photopic images are generally too bright and detailed." (Noted by 3 observers)
—"Street lights and gallery lights are expected to be turned on in a realistic night scene."
—"Too much depth doesn't look similar to scotopic conditions."
—"More depth in a video game is always preferred."
—"Our method looks more similar to scotopic for the Art Gallery."

As a control group, monocular day-for-night and unprocessed images were shown asking the same questions. The only significant result was that day-for-night was more similar to scotopic conditions than the unprocessed image in all scenes (all $p < .02$). Comments made were:

—"Unprocessed color doesn't look similar to scotopic."
—"The blue shift makes it appear more scotopic."
—"Day-for-night is less blurry than scotopic."
—"The unprocessed image looks more similar to scotopic, except for color."

The overall mixed outcome is expected as stereo perception preferences are already highly subjective and even more so in scotopic conditions. While strictly speaking we cannot conclude anything from insignificance, the outcome shows that while day-for-night has been accepted for many decades this did not result in a clear user preference, both for classic monocular and our stereo approach.

9. CONCLUSION AND FUTURE WORK

In this work we analyzed the relation of luminance adaptation and stereo perception. We conducted perceptual experiments to cover a very large range of luminance in stereo and devised a model that relates luminance contrast and luminance adaptation to disparity threshold elevation. This model was used to process binocular disparity, such that photopic stereo appearance is matched to the scotopic one. This processing can be achieved in real-time and is designed to extend classic day-for-night tone mapping in the luminance domain to stereo, e. g., in a computer game that should to convey a nocturnal mood.

The model represents a true-to-life simulation of the visual degradation due to reduced information in scotopic conditions. Viewers may not prefer to be visually impaired in movies or video games, but do like a convincing depiction of scotopic conditions. Our scotopic stereo is a tool at the disposal of the director to make a scene feel more nocturnal.

Our day-for-night technique filters the disparities based on the model fitted to our measurements, essentially removing small depth details and compressing the depth range. As future work we would like to investigate simpler models that could produce similarly reduced stereo perception with lower implementation complexity. We also would like to better understand the relation of scotopic depth perception and suprathreshold disparity, chroma, the time course of adaptation as well as different disparity frequencies, for which we do not account in this work.

ACKNOWLEDGMENT

We would like to thank Rafał Mantiuk for helpful discussion and the reviewers for insightful comments. The project was partially supported by the European Cooperation in Science and Technology ICT COST Action IC1005.

REFERENCES

BANKS, M. S., GEPSHTEIN, S., AND LANDY, M. S. 2004. Why is spatial stereoresolution so low? *J Neuroscience 24,* 9, 2077–89.

BURT, P. J. AND ADELSON, E. H. 1983. The laplacian pyramid as a compact image code. *IEEE Trans. Comm. 31,* 4, 532–40.

CORMACK, L., STEVENSON, S., AND SCHOR, C. 1991. Interocular correlation, luminance contrast and cyclopean processing. *Vis. Res. 31,* 12, 2195–207.

DIDYK, P., RITSCHEL, T., EISEMANN, E., MYSZKOWSKI, K., AND SEIDEL, H.-P. 2011. A perceptual model for disparity. *ACM Trans. Graph. (Proc. SIGGRAPH) 30*, 96:1–96:10.

DIDYK, P., RITSCHEL, T., EISEMANN, E., MYSZKOWSKI, K., SEIDEL, H.-P., AND MATUSIK, W. 2012. A luminance-contrast-aware disparity model and applications. *ACM Trans. Graph. (Proc. SIGGRAPH Asia) 31,* 6, 184:1–184:10.

DURAND, F. AND DORSEY, J. 2000. Interactive tone mapping. In *Proc. EGWR*. Eurographics, 219–230.

FEHN, C. 2004. Depth-image-based rendering (DIBR), compression, and transmission for a new approach on 3D-TV. In *Proc. SPIE.* 93–104.

FERWERDA, J. A., PATTANAIK, S., SHIRLEY, P., AND GREENBERG, D. P. 1996. A model of visual adaptation for realistic image synthesis. In *Computer Graphics (Proc. SIGGRAPH)*. ACM, 249–58.

FILIPPINI, H. R. AND BANKS, M. S. 2009. Limits of stereopsis explained by local cross-correlation. *J Vis. 9,* 1, 1–18.

FRISBY, J. AND MAYHEW, J. 1978. Contrast sensitivity function for stereopsis. *Perception 7*, 423–9.

HARO, G., BERTALMÍO, M., AND CASELLES, V. 2006. Visual acuity in day for night. *Int. J. Comput. Vision 69,* 1, 109–117.

HECKMANN, T. AND SCHOR, C. M. 1989. Is edge information for stereoacuity spatially channeled? *Vis Res 29,* 5, 593–607.

HESS, R., SHARPE, L., AND NORDBY, K. 1990. *Night Vision: Basic, Clinical and Applied Aspects*. Cambridge University Press.

HOFFMAN, D., GIRSHICK, A., AKELEY, K., AND BANKS, M. 2008. Vergence-accommodation conflicts hinder visual performance and cause visual fatigue. *J. Vision 8,* 3, 1–30.

KELLNHOFER, P., RITSCHEL, T., MYSZKOWSKI, K., AND SEIDEL, H.-P. 2013. Optimizing disparity for motion in depth. *Comp. Graph. Forum (Proc. EGSR) 32,* 4, 143–152.

KIRK, A. G., , AND O'BRIEN, J. F. 2011. Perceptually based tone mapping for low-light conditions. *ACM Trans. Graph. (Proc. SIGGRAPH) 30,* 4, 42:1–10.

KUANG, J., JOHNSON, G. M., AND FAIRCHILD, M. D. 2007. iCAM06: A refined image appearance model for HDR image rendering. *J Vis Comm Image Repr. 18,* 5, 406–414.

LAMBOOIJ, M., IJSSELSTEIJN, W., FORTUIN, M., AND HEYNDERICKX, I. 2009. Visual discomfort and visual fatigue of stereoscopic displays: A review. *J. Imaging Sci. Technol. 53,* 3, 1.

LANG, M., HORNUNG, A., WANG, O., POULAKOS, S., SMOLIC, A., AND GROSS, M. 2010. Nonlinear disparity mapping for stereoscopic 3D. *ACM Trans. Graph. (Proc. SIGGRAPH) 29,* 4, 75:1–75:10.

LEGGE, G. AND GU, Y. 1989. Stereopsis and contrast. *Vis Res 29,* 8, 989–1004.

LIT, A. 1959. Depth-discrimination thresholds as a function of binocular differences of retinal illuminance at scotopic and photopic levels. *J. Opt. Soc. Am. 49,* 8, 746–752.

LIT, A. AND HAMM, H. D. 1966. Depth-discrimination thresholds for stationary and oscillating targets at various levels of retinal illuminance. *J. Opt. Soc. Am. 56,* 4, 510–514.

LIVINGSTONE, M. 2002. *Vision and Art: The Biology of Seeing*. Harry N. Abrams.

LIVINGSTONE, M. S. AND HUBEL, D. H. 1994. Stereopsis and positional acuity under dark adaptation. *Vis. Res. 34,* 6, 799–802.

MANTIUK, R., KIM, K. J., REMPEL, A. G., AND HEIDRICH, W. 2011. Hdr-vdp-2: A calibrated visual metric for visibility and quality predictions in all luminance conditions. *ACM Trans. Graph. (Proc. SIGGRAPH) 30,* 4, 40:1–40:14.

MANTIUK, R., MYSZKOWSKI, K., AND SEIDEL, H.-P. 2006. Lossy compression of high dynamic range images and video. In *Human Vision and Electronic Imaging XI, IS&T/SPIE Symposium on Electronic Imaging*. IS&T/SPIE, 60570V.

O'SHEA, R. P., BLAKE, R., AND WOLFE, J. M. 1994. Binocular rivalry and fusion under scotopic luminances. *Perception 23,* 7, 771–784.

PATEL, S. S., BEDELL, H. E., TSANG, D. K., AND UKWADE, M. T. 2009. Relationship between threshold and suprathreshold perception of position and stereoscopic depth. *J Opt Soc Am A 26,* 4, 847–861.

PATTANAIK, S. N., TUMBLIN, J. E., YEE, H., AND GREENBERG, D. P. 2000. Time-dependent visual adaptation for fast realistic image display. In *Proc. SIGGRAPH*. ACM, 47–54.

QIN, D., TAKAMATSU, M., AND NAKASHIMA, Y. 2006. Disparity limit for binocular fusion in fovea. *Optical Review 13,* 1, 34–38.

REINHARD, E., WARD, G., DEBEVEC, P., PATTANAIK, S., HEIDRICH, W., AND MYSZKOWSKI, K. 2010. *High Dynamic Range Imaging*. Morgan Kaufmann Publishers, 2nd edition.

SCHARSTEIN, D. AND PAL, C. 2007. Learning conditional random fields for stereo. In *CVPR*. IEEE Computer Society.

SHLAER, S. 1937. The relation between visual acuity and illumination. *J Gen Phys 21*, 165–188.

SIMMONS, D. R. AND KINGDOM, F. A. A. 1997. On the independence of chromatic and achromatic stereopsis mechanisms. *Vision Research 37,* 10, 1271–1280.

SIMMONS, D. R. AND KINGDOM, F. A. A. 2002. Interactions between chromatic- and luminance-contrast-sensitive stereopsis mechanisms. *Vision Research 42,* 12, 1535–1545.

SUBR, K., BRADBURY, G., AND KAUTZ, J. 2012. Two-frame stereo photography in low-light settings: A preliminary study. In *Proc. CVMP*. ACM, 84–93.

THOMPSON, W. B., SHIRLEY, P., AND FERWERDA, J. A. 2002. A spatial post-processing algorithm for images of night scenes. *J Graphics Tools 7,* 1, 1–12.

WANDELL, B. A. 1995. *Foundations of Vision*. Sinauer Associates.

WARD, G., RUSHMEIER, H., AND PIATKO, C. 1997. A visibility matching tone reproduction operator for high dynamic range scenes. *IEEE Trans. Vis. and Comp. Graph. 3,* 4, 291–306.

WATSON, A. B. AND PELLI, D. G. 1983. QUEST: a bayesian adaptive psychometric method. *Perception & Psychophysics 33,* 2, 113–120.

WHEATSTONE, C. 1838. Contributions to the physiology of vision.–Part the first. On some remarkable, and hitherto unobserved, phenomena of binocular vision. *Phil Trans. Royal Society of London 128*, 371–394.